Dry and Noncontact EEG Sensors for Mobile Brain–Computer Interfaces

Yu Mike Chi, *Member, IEEE*, Yu-Te Wang, Yijun Wang, Christoph Maier, *Member, IEEE*, Tzyy-Ping Jung, *Senior Member, IEEE*, and Gert Cauwenberghs, *Fellow, IEEE*

***Abstract*—Dry and noncontact electroencephalographic (EEG) electrodes, which do not require gel or even direct scalp coupling, have been considered as an enabler of practical, real-world, brain–computer interface (BCI) platforms. This study compares wet electrodes to dry and through hair, noncontact electrodes within a steady state visual evoked potential (SSVEP) BCI paradigm. The construction of a dry contact electrode, featuring fingered contact posts and active buffering circuitry is presented. Additionally, the development of a new, noncontact, capacitive electrode that utilizes a custom integrated, high-impedance analog front-end is introduced. Offline tests on 10 subjects characterize the signal quality from the different electrodes and demonstrate that acquisition of small amplitude, SSVEP signals is possible, even through hair using the new integrated noncontact sensor. Online BCI experiments demonstrate that the information transfer rate (ITR) with the dry electrodes is comparable to that of wet electrodes, completely without the need for gel or other conductive media. In addition, data from the noncontact electrode, operating on the top of hair, show a maximum ITR in excess of 19 bits/min at 100% accuracy (versus 29.2 bits/min for wet electrodes and 34.4 bits/min for dry electrodes), a level that has never been demonstrated before. The results of these experiments show that both dry and noncontact electrodes, with further development, may become a viable tool for both future mobile BCI and general EEG applications.**

***Index Terms*—Brain–computer interface (BCI), capacitive electrodes, dry electrodes, electroencephalographic (EEG), noncontact electrodes, steady state visual evoked potential (SSVEP).**

Manuscript received May 02, 2011; revised August 01, 2011; accepted October 15, 2011. Date of publication December 12, 2011; date of current version March 16, 2012. This work was supported in part by the Defense Advanced Research Projects Agency (DARPA), in part by the National Science Foundation (NSF), in part by Telemedicine and Advanced Technology Research Center (TATRC), in part by the Army Research Laboratory, in part by the Army Research Office, in part by the Office of Naval Research, in part by the National Semiconductor, in part by the Chan Soon-shiong Scholar program, and in part by the Institute for Engineering in Medicine.

Y. M. Chi was with the Department of Electrical and Computer Engineering, Jacobs School of Engineering, University of California-San Diego, La Jolla, CA 92093 USA. He is now with Cognionics, Inc., San Diego, CA 92121 USA (e-mail: mike@cognionics.com).

Y.-T. Wang, Y. Wang, and T.-P. Jung are with the Institute for Neural Computation, University of California-San Diego, La Jolla, CA 92093 USA, and also with the Institute of Engineering in Medicine, University of California-San Diego, La Jolla, CA 92093 USA.

C. Maier and G. Cauwenberghs are with the Department of Bioengineering, Jacobs School of Engineering, University of California-San Diego, La Jolla, CA 92093 USA, and also with the Institute for Neural Computation, University of California-San Diego, La Jolla, CA 92093 USA.

Color versions of one or more of the figures in this paper are available online at http://ieeexplore.ieee.org.

Digital Object Identifier 10.1109/TNSRE.2011.2174652

I. Introduction

BRAIN–COMPUTER interfaces (BCIs) have been an area of intense study both as a means to rehabilitate injured patients and to simply augment the standard tactile, mechanical user interfaces ubiquitous today. Despite remarkable advancements in both neuroscience, signal processing algorithms and portable computing devices [1], [2], the promise of a practical, user-friendly, noninvasive, and mobile EEG-based BCI platform has remained elusive. Conventional BCI systems have always relied on laboratory bound instrumentation [3]–[7] and often require extensive subject preparation, including scalp abrasion, gels and a multitude of wired electrodes. Thus, the unassisted use of EEG-based BCI systems, outside the laboratory, is still a difficult proposition. For truly mobile BCI systems to become a reality, significant improvements in the sensor hardware are still needed.

In light of these limitations with the actual physical sensor interface, extensive research has produced a huge variety of dry electrodes ranging from simple metal discs [8], conductive rubber [9], conductive carbon nanotubes [10], [11], micro-machined structures [12]–[18], spring-loaded fingers [19], [20] to conductive foam [21]. Despite the multitude of options in the literature, however, detailed knowledge regarding the performance of dry electrodes for BCI is sparse. In particular, there exists no objective metrics and only a few studies exist directly comparing dry versus wet electrodes [9], [22], [23].

With an aim towards advancing the understanding and use of dry/noncontact EEG electrodes, this paper focuses on quantifying their performance within a BCI paradigm. The dry sensor tested is a simple active electrode built from standard off-the-shelf electronic components. Spring loaded fingers [24] provide for electrical connection to the scalp by pushing through the strands of hair. High contact impedances from the absence of gel and the small contact surface are mitigated with the use of an onboard buffer. The noncontact sensor design is a novel, high-impedance, noncontact electrode design based on a custom integrated analog front-end. Noncontact electrodes have been explored for ECG use and more rarely, EEG as well [25], [26]. However, the signal quality requirements are far more stringent for EEG than ECG, and the prototype sensors built from standard off-the-shelf components have been, to date, limited by noise and usability issues [8]. In contrast, our recent work has demonstrated a fully custom sensor front-end that is able to bypass many of the input impedance, noise and biasing issues encountered in previous works. Detailed characterization of the this new integrated sensor can be found in the literature [27].

A mobile, wireless SSVEP BCI framework [2] serves as the basis for our experiments in this study. Visual evoked potential measurements serve as a convenient benchmark since SSVEP signals are well-defined and repeatable. Data taken with the three types of electrodes (wet, dry, and noncontact) show the potential for dry electrodes to be fully usable for wireless BCI applications. While the signal quality from the integrated noncontact electrode still shows degradation as compared to its wet and dry counterparts, the experiments in this paper further suggest the possibility of realizing a mobile, noncontact through hair BCI system.

II. Wireless Dry/Noncontact EEG System Design

A. Discrete Dry Sensor

The dry sensor consists of two sections. A lower plate contains a set of spring-loaded pin contacts which can easily penetrate hair without the need for any preparation. The gold plated "fingers" achieve direct electrical connection to the scalp. A male snap connector (identical to the one used for ECG electrodes) on the top side of the plate mates with it's female counterpart on a second PCB which contains the active electrode circuitry. A detailed picture of the circuit board along with the fingered electrodes can be found in Fig. 2.

Relatively high impedance signals offered by the dry contact are buffered with an off-the-shelf CMOS-input opamp (National Semiconductor LMP7702). The unity gain buffer, along with the shielded cabling, greatly reduces the effects of external interference.

As will be shown, the signal quality from this very simple dry electrode is excellent, and does not require any preparation. Compared to the wet electrode, a significantly greater amount of low-frequency drift was present, likely due the high contact impedance and the less stable electrochemical interface of the Au pins versus the normal Ag/AgCl electrode. Nevertheless, these effects were easily removed and far below SSVEP frequencies of interest. No discomfort was observed during usage. It is worthwhile to note, however, that the fingers may present an injury hazard in cases of direct head trauma, inspiring the development of the noncontact sensors described below.

B. Integrated Noncontact Sensor

As previously mentioned, noncontact electrodes which operate primarily via capacitive coupling have been studied for various applications, including EEG [28], [26]. Although the impedance of dry scalp based electrodes are still relatively easy to handle with active electrodes using standard CMOS amplifiers, the extremely high contact impedance $(> 10\,\mathrm{G\Omega}||30\,\mathrm{pF})$, in the same order of magnitude as even the best CMOS-input amplifiers, of through-hair coupling has been a significant challenge in acquiring acceptable EEG signals. The attenuation due to source-input impedance division significantly degrades the CMRR of the front-end amplifiers. In addition, the high impedance interface can also, in many cases, generate significant amounts of intrinsic noise and is susceptible to various movement artifacts and microphonics [8], [29].

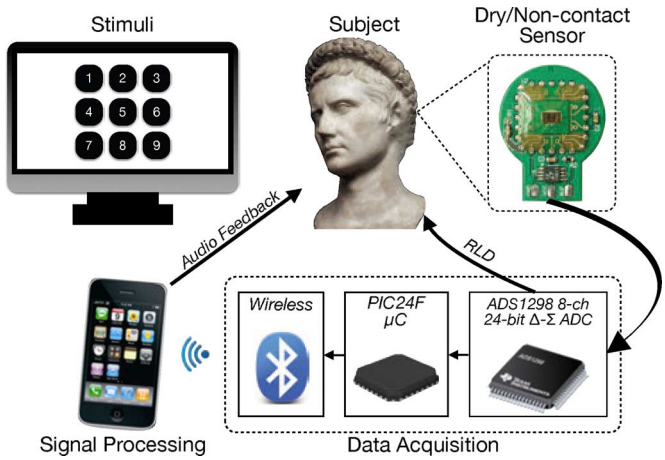

Fig. 1. Wireless dry/noncontact BCI system concept. The BCI interface consists of a computer based visual stimulus program. SSVEP/EEG signals are acquired using dry/noncontact electrodes embedded within a headband over the hair in the occipital region. A high-resolution data acquisition system relays EEG telemetry to a cellular phone which decodes the SSVEP signals.

The new integrated sensor (Fig. 3) achieves it's high input impedance through careful design and control of the sensitive input node, made possible by the custom VLSI circuit implementation. Previous attempts at building noncontact sensors have always relied on active shielding to minimize noise and interference, but the shield's effectiveness was necessarily constrained to the PCB-level due to the lack of access to the internal nodes of the off-the-shelf amplifiers used in the front-end. Any parasitic capacitances internal to the amplifier (≈2–20 pF) still had to be eliminated via manually tuned neutralization networks. Not only is this calibration process imperfect, it also precludes the mass production of these sensors. In contrast, we were able to fully bootstrap and shield the input node, starting from the active transistor, extending out to the bondpads and out to a specially constructed chip package. A detailed description and characterization of the noncontact front-end can be found in another publication [30].

C. Reference Wet Electrode

A set of standard passive hydrogel ECG electrodes were used as a control in the experiments. The adhesive sections of the electrodes were removed, leaving only the hydrogel which was placed on top of the subject's hair. Additional conductive gel was dispensed to ensure a good electrical connection to the scalp. No special preparation of the skin, such as abrasion, was required. The low-impedance of the wet electrode, even without any active buffering circuitry, exhibited the best signal quality in terms of noise and drift.

D. Wireless Data Acquisition

Each of the sensors are connected directly to an octal, simultaneous sampling 24-bit $\Delta\Sigma$ ADCs (TI ADS1298). The ADC is controlled by a PIC24F low-power microcontroller which acquires samples and dispatches the data to an onboard Bluetooth module (Fig. 1). The portable data acquisition box is powered by two AAA batteries, good for approximately 10 h of continuous wireless telemetry.

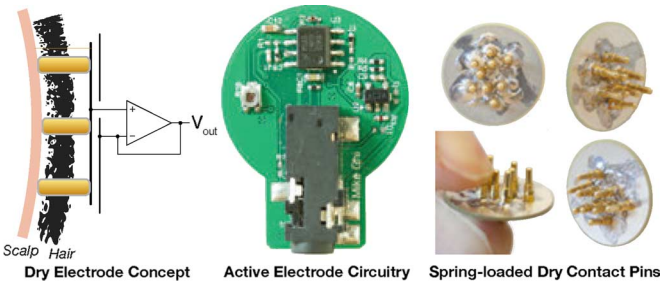

Fig. 2. The implemented dry contact electrode used in the experiments. Spring-loaded pins push through the subject's hair and make contact with the scalp. The plate embedding the pins snaps into a buffer circuitry which provides a low-impedance output to the data acquisition box.

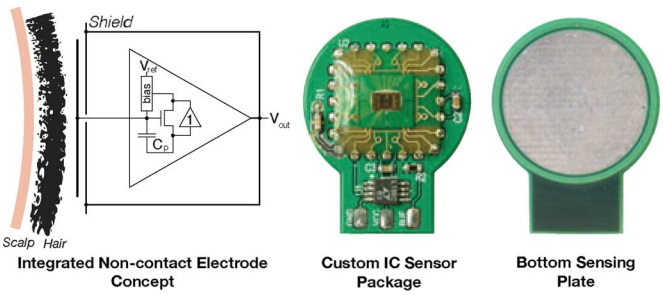

Fig. 3. Diagram and picture of the integrated noncontact electrode [27], which operates on top of hair. The integrated electrode achieves input impedances much greater than what has been possible with discrete designs through careful shielding and custom packaging made possible with an fully custom IC design.

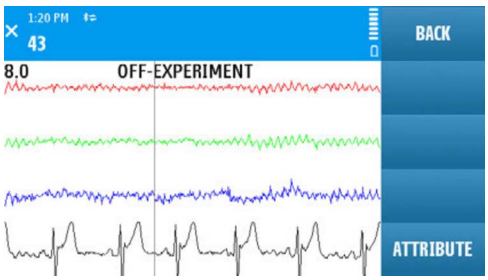

Fig. 4. Picture of the GUI interface on the cellular phone displaying sample data (0–50 Hz BW) from three noncontact electrodes, over hair, transmitted for display on a cellular phone. A reference ECG signal, taken with a standard wet electrode on the chest, is also displayed. Data processing occurs in real-time on the mobile device.

E. Mobile Signal Processing

Signal processing of the EEG telemetry was accomplished on a Nokia N97 cellular phone. A sample plot of alpha wave activity, displayed on the phone's 640 × 360 pixel 3.5 in touchscreen LCD, from three noncontact electrodes is shown in Fig. 4. The BCI application was written in J2ME (Java 2 Micro Edition) using JBuilder 2005.

The phone establishes a Bluetooth serial port connection with the data acquisition box and initially presents the user with raw telemetry (Fig. 4). After the EEG signal quality has been visually inspected by the user to be suitable for an experiment, the application can switch to canonical correlation analysis (CCA) mode for actual BCI experimentation. In the analysis mode, a band-pass filter is applied to the signal to remove frequencies that are outside the SSVEP band (9–12 Hz).

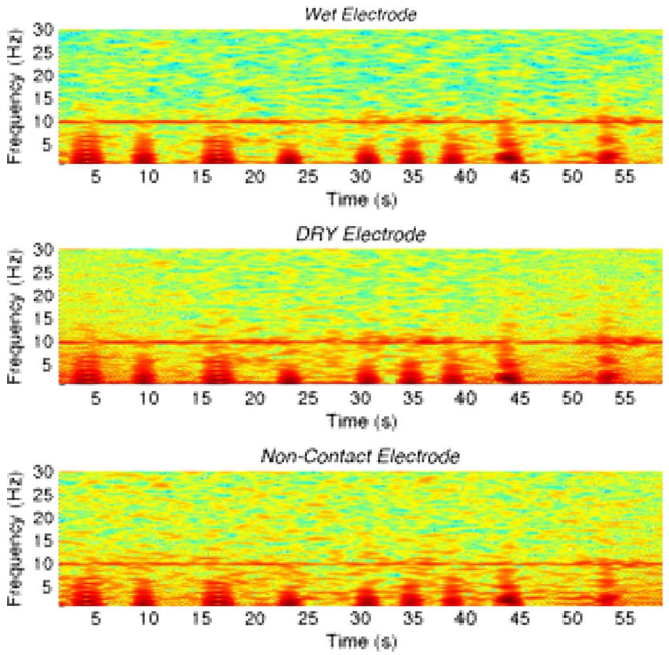

Fig. 5. Spectrogram of one 60 s trial for subject two. The 10 Hz SSVEP stimulus tone is visible in the spectra of the signals from every electrode. Blink artifacts are also visible.

The CCA analysis algorithm [2] attempts to obtain the maximum correlation between the signal from the three recording electrodes and a matrix of templates corresponding to the SSVEP stimulus frequencies. As will be explained in greater detailed, the online portion of the study involves a BCI with 12-possible selections corresponding to a number pad. Thus there are 12 SSVEP stimuli each with a corresponding template that is matched against the EEG signal. For the experiments involving wet and dry electrodes, decisions are made on a 4 s sliding window that advances in 1 s increments. Two consecutive decisions are construed as a successful input and trigger an audio feedback to notify the subject. To allow the subject time for rest and blinks, a 1 s blackout is enforced after each input. During the tests, it was found that the 4 s window with two consecutive decisions was not reliable enough for the noncontact electrodes due to degraded SNR. Increasing the window to 6 s with four consecutive decisions allowed for sufficient rejection of the extra noise.

III. Comparative SSVEP Sensor Benchmark

To first validate the signal being acquired by the dry and noncontact sensors compared to the standard wet Ag/AgCl electrode, a comparative experiment was devised and performed on ten different subjects. The experiment consisted of having each subject gaze at a single SSVEP target stimulus, displayed on a CRT monitor, at 10 Hz for a 1-min duration. During the experiment, the SSVEP signal was decoded, in real-time, to verify the presence of the 10 Hz stimulus signal, but no feedback was presented to the subject. Each subject repeated this task three times, and the best dataset was used for analysis. None of the subjects had shaved heads and in all cases, the noncontact sensor was on top of several layers of hair.

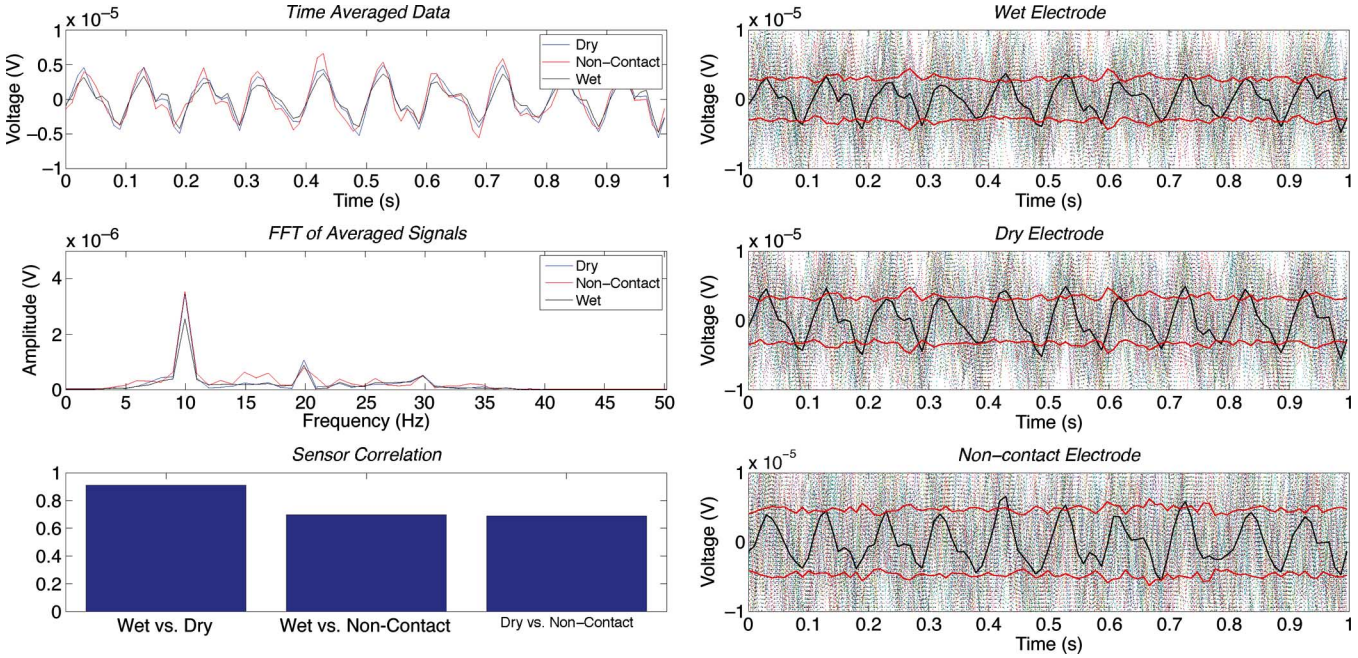

Fig. 6. (Left) Sample time averaged SSVEP signals from the wet, dry, and noncontact electrodes for one subject during a 60 s trial along with the FFT and correlation. Averaging was performed over a 1 s period using a 0.5 s sliding window. (Right) Detailed signals from each electrodes with the average in black, the standard deviation in red along with the raw signals.

A. *Comparative Benchmark Results*

Directly benchmarking several EEG sensors on a live subject can be problematic. Unlike ECG where there exists large areas at an equipotential (e.g., limbs), even closely spaced EEG electrodes may not always observe the exact same signal. In this experiment the three sensors (wet, dry, and noncontact), were arrayed in a triad over the occipital region as closely together as possible. The relative placement of the electrodes was consistent between different subjects. Care was taken to prevent gel from the wet electrode seep into the neighboring dry and noncontact electrodes.

The spectrogram (Fig. 5) of the signal acquired from each sensor during one of the 60 s trials show that the SSVEP stimulus can be acquired by all three sensors. A detailed plot of the raw and time averaged SSVEP signal is also shown in Fig. 6 along with the PSD in Fig. 7. In the four subjects shown in the figures, the 10 Hz stimulus is clearly visible, although the amplitude of the SSVEP and amount of the background "noise" varies considerably between subjects. From first glance, the PSD from the wet electrode almost perfectly matches that from the dry electrode, consistent from our observations that aside from larger amounts of drift, the signal quality from the dry electrode was excellent. The PSD of the noncontact electrode's signal also clearly shows the 10 Hz stimulus, verifying that it is indeed capable of acquiring EEG signals through hair. Unlike the dry electrode, the noncontact sensor can exhibit a greater amount of both low-frequency drift as well as broadband noise due to the extremely high coupling impedance and sensitivity to movement artifacts. In one subject (Fig. 7 bottom left) a pulse artifact can be seen in the spectra due to poor coupling of the noncontact electrode.

For quantitative analysis of the signal quality from the various electrode types, a few key parameters are desired. First, it is useful to obtain a metric that conveys how close the signal from dry and noncontact electrodes matches the signal from a "gold standard" wet electrode. Secondly, it is also useful to calculate the ratio of signal versus noise (SNR) for each of the sensors.

Specifically for this experiment, the three sensor were first band-pass filtered around 8–13 Hz to remove all frequencies not relevant to the SSVEP stimulus. Since the SSVEP signal is small, this removes the majority of noise in the signal and enables a correlation comparison between the three sensors specifically for the SSVEP paradigm. To account for phase shifts of the SSVEP signal due to differences in electrode placement, the cross correlation (MATLAB *xcorr*) was used, and the maximum value was extracted for three comparsions: wet versus dry, wet versus noncontact, and dry versus noncontact. A summary of the computed correlations can be found in Table I.

For the dry electrode, over half the subjects had a correlation of greater than 0.9 between the wet and dry electrodes, with three subjects achieving almost perfect correlation (0.978, 0.967, 0.975). Only one subject exhibited a wet versus dry electrode correlation of less than 0.8. Correlation values of the wet versus noncontact electrode were lower, which was not surprising. Nevertheless, half the subjects had correlation values of above 0.8. Only one subject had a correlation value of less than 0.7.

Previous studies [9], [22] of dry electrodes typically found correlation values of approximately 0.8 between neighboring wet and dry electrodes. It is important to note, however, that the experiments in this paper are narrow band in nature (8–13 Hz), whereas previous studies were focused on more general EEG experiments with larger signal bandwidths. This discrepancy in bandwidth makes an direct, objective comparison difficult.

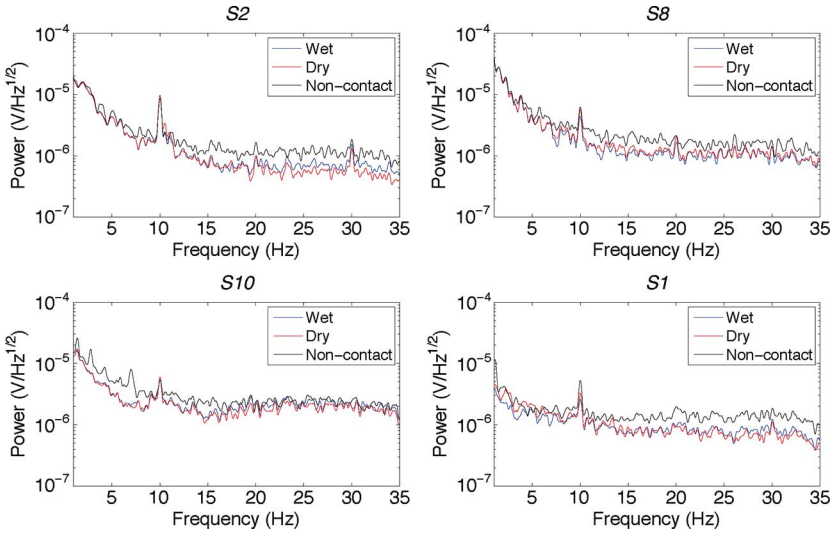

Fig. 7. Power spectral density of the simultaneously acquired EEG signal with the wet, dry, and noncontact electrodes as the subject was asked to gaze at the 10 Hz stimulus target. The PSD was computed over a continuous 60 s period.

TABLE I
SIGNAL CORRELATION BETWEEN DIFFERENT ELECTRODES

Subject	SSVEP Amplitude (μV)			Sensor Correlation			SNR (dB)		
	Wet	Dry	NC	Wet vs. Dry	Wet vs. NC	Dry vs. NC	Wet	Dry	NC
1	1.1	1.7	2.2	0.88	0.85	0.74	-15.16	-10.97	-10.36
2	3.7	3.7	3.2	0.98	0.88	0.85	-6.49	-7.00	-8.46
3	1.9	2.0	2.1	0.90	0.78	0.70	-11.71	-12.24	-12.96
4	2.2	2.2	2.4	0.97	0.80	0.78	-7.69	-8.09	-8.22
5	1.1	1.1	1.0	0.97	0.96	0.94	-12.24	-11.87	-13.05
6	1.6	1.2	1.4	0.75	0.71	0.55	-6.61	-10.49	-9.67
7	1.6	1.1	1.8	0.91	0.86	0.88	-14.33	-13.61	-10.72
8	2.5	3.4	3.5	0.93	0.73	0.70	-6.85	-5.17	-7.47
9	1.4	0.8	0.8	0.89	0.85	0.85	-13.08	-17.42	-17.64
10	1.4	1.8	1.4	0.95	0.57	0.59	-15.60	-13.29	-18.21
Mean	**1.8**	**1.9**	**2.0**	**0.91**	**0.80**	**0.76**	**-10.98**	**-11.01**	**-11.68**
STD	0.8	1.0	0.9	0.07	0.11	0.13	3.71	3.56	3.78

TABLE II
SENSOR CORRELATION OVER DIFFERENT FREQUENCIES

	Frequency Band									
	2-30Hz		2-4Hz		4-8Hz		8-12Hz		12-30Hz	
	Mean	STD	Mean	STD	Mean	STD	Mean	STD	Mean	STD
Wet vs Dry	0.92	0.09	0.92	0.13	0.93	0.09	0.91	0.07	0.88	0.08
Wet vs NC	0.80	0.15	0.79	0.22	0.77	0.16	0.80	0.11	0.77	0.12
Dry vs NC	0.76	0.18	0.74	0.25	0.72	0.19	0.76	0.12	0.73	0.13

To help facilitate objective comparisons, not just for SSVEP paradigms, we have additionally computed the correlation over different sub-bands (Table II). In general, the correlation is fairly consistent irrespective of the bandwidth of interest. At very low frequencies (<1 Hz), however, the correlation comparison becomes skewed due to drift noise. Drift, such as sweat artifacts, typically have very large amplitudes. Depending on where the drift was occurring—either at the reference electrode (common) or the recording electrode, the results can be very different. As an example, if the two electrodes were drifting independently, then the correlation value would decrease towards zero. On the other hand, if the common reference electrode was in poor contact and noisy, causing the two recording electrodes to drift synchronously, then the correlation value will increase towards one, irrespective of how well the individual sensors are performing.

The second metric, SNR, was computed by examining the root-mean square amplitude of the fundamental 10 Hz tone, obtained via an FFT on the time averaged data ($\bar{X}$), versus the background noise within the 8–13 Hz SSVEP band

$$\mathrm{SNR} = 10\ \log_{10} \frac{\bar{X}(10\ \mathrm{Hz})^2_{\mathrm{rms}}}{var(x) - \bar{X}(10\ \mathrm{Hz})^2_{\mathrm{rms}}}. \qquad (1)$$

The background noise was approximated by subtracting out the contribution from the SSVEP tone from the standard deviation of the 8–13 Hz band-passed EEG (x) signal during the 60 s trial. This allows for a direct comparison of the signal strength versus noise for each electrode. This number, provided in Table I, represents the instantaneous SNR and is always well below 0 dB due to the small amplitude of the SSVEP signal relative to the

TABLE III
RESULTS FROM ONLINE BCI TESTS

		Accuracy			Detection Time (s)			ITR (bits/min)		
		Wet	Dry	NC	Wet	Dry	NC	Wet	Dry	NC
Subject 1	Trial 1	0.83	0.92	1.00	6.2	5.7	10.3	23.0	28.1	19.3
	Trial 2	0.83	0.83	1.00	5.9	5.8	9.7	23.9	22.6	20.5
	Trial 3	0.83	1.00	1.00	6.4	5.6	9.4	20.5	34.4	21.0
Subject 2	Trial 1	0.83	0.83	0.50	6.2	5.9	12.8	23.0	23.9	4.0
	Trial 2	0.83	0.92	0.75	5.9	6.3	9.7	23.9	27.3	11.9
	Trial 3	0.92	0.83	0.75	5.7	6.3	11.0	29.2	22.6	10.4
	Mean	**0.85**	**0.89**	**0.83**	**6.04**	**5.92**	**10.49**	**23.9**	**26.5**	**14.5**
	STD	0.03	0.07	0.20	0.26	0.31	1.29	2.90	4.52	6.85

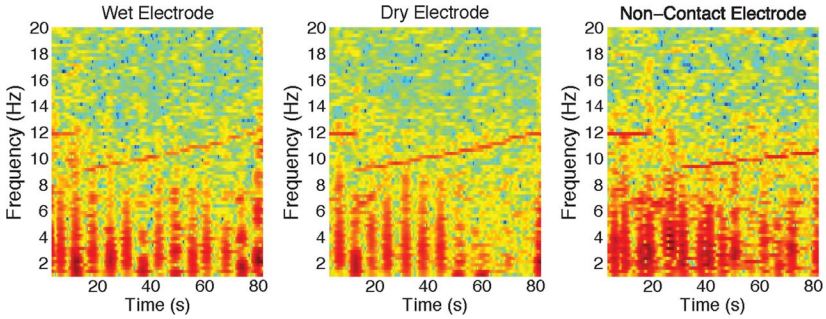

Fig. 8. Exemplary spectrograms of the SSVEP data taken during the online tests for each of the three electrodes. The different SSVEP test frequencies (8–12 Hz) are clearly visible as the subject switches targets. The spectrogram of wet and dry sensors are similar. The SSVEP signal is also clearly visible in the noncontact trial, although there is greater background energy due to the higher noise floor of the sensor. Additionally each frequency step is of a longer duration, corresponding to the increased window used for the noncontact sensor.

background EEG and noise. Reliable detection of the stimulus, however, is made possible by the processing gain from FFT or CCA analysis of the signal over a time window.

IV. REAL-TIME DECODING OF NONCONTACT SSVEP SIGNALS

Offline analysis of benchmark data shows that SSVEP signals can be reliably extracted from dry and even noncontact electrodes. To demonstrate their use in real-time BCI applications, subjects 1 and 2 were recalled to perform an SSVEP phone dialing task using the mobile signal processing platform. Subjects 1 and 2 were selected for the online test due to their ability to be highly compliant with the experimental protocol. As both SSVEP stimulus system and EEG hardware become more robust, it will be highly useful to run wider tests beyond this baseline pilot study. Additional details regarding this SSVEP paradigm can be found in a previous publication [2].

The online task consisted of entering a predetermined 12-digit sequence. The time to complete the task along with the error rate was recorded and used to calculate the ITR [2], [31], which is a metric that relates the accuracy of the BCI versus the time required for the task. Signal decoding was performed using CCA analysis on data streamed across the wireless link. A full suite of tests was conducted on subjects 1 and 2 which consisted of using all three of the electrode types in multiple separate trials. Data from the tests is shown in Table III. Fig. 8 shows the Subject 1's spectrograms from each of the trials for the three different electrodes The different SSVEP frequencies are clearly visible as the subject performs the dialing task.

Both subjects were able to achieve control of the BCI system using any electrode type. As expected, the wet and dry electrodes were could both be successfully used for BCI, although with a minor error rate, typically 1 or 2 errors out of 12. Although the ITRs in this experiment do not quite match the best of previous reports in the literature, it does provide for a baseline in this comparative study. It is possible that higher ITRs could be achieved if more electrodes were available—in the current experiment, only three electrodes are used at a time. It is interesting to note that the dry electrode trials actually achieved superior performance to the wet electrode trials. This is likely attributed to the fact that the wet electrode was always tested last (to avoid gel contamination on the dry and noncontact sensors). Subject fatigue and variability may have a significant performance impact over time. Nevertheless, this establishes the feasibility of dry electrodes for SSVEP BCI use.

With the non contact electrodes, one of the subjects (1) was able to consistently achieve 100% accuracy. Although a longer detection window was required to compensate for the increased noise with noncontact electrodes, we were able to achieve an ITR of over 19 bits/min. The lower speed of the BCI, from the increased window length, resulted in an effectively lower ITR, which is a metric that is proportional to the accuracy divided by speed of the BCI [2]. To our knowledge, this level of performance with noncontact electrodes has never been demonstrated before. The only previous study of true noncontact, capacitive BCI achieved an ITR of 12.5 bits/min [26], which required both a training session and the use of significantly less selection choices (3 versus the 12 in our study). Even though additional study is clearly warranted, this is strong indicator that the new integrated noncontact electrodes do indeed acquire useful EEG.

Subject 2 had more difficulty with utilizing the noncontact electrodes, probably a result of thicker hair which made the sensors more susceptible to motion artifacts. Movement induced errors were a challenge in subject 2's trial since the SSVEP paradigm requires a stable signal over a time window (4–6 s). Transient artifacts appear as a large 1/f disturbance in the frequency domain and can cause either decoding errors and/or excessively long decision times.

An interesting dichotomy was noted during the experiments. Whereas wet electrodes typically perform well shortly after application (allowing for a short time to stabilize the electrochemical interface), the dry and noncontact electrodes take much longer to achieve a stable trace. On the other hand, wet electrodes are susceptible to drying of the electrogel over time, but the signals from dry and noncontact electrodes do not degrade with time. This is likely due to sweat and other effects moisturizing the hair and skin under the electrode, achieving improved coupling. While this phenomenon with dry and noncontact electrodes is disadvantageous in time constrained laboratory applications, it may become useful for long-term, mobile use.

V. Conclusion

As further improvements in both neuroscience and signal processing better enable better EEG applications, including BCI, there exists a need for sensor arrays that do not require time and labor intensive preparation to truly transition laboratory innovations into general use. With that goal in mind, dry and noncontact electrodes offer a potential solution that may alleviate many of usability shortcomings inherent with wet electrodes.

Quantitative benchmarking show that dry and noncontact electrodes are capable of resolving SSVEP-type signals. In many cases, the dry electrode only shows a slight amount of signal degradation, except for increased drift, compared to the standard wet Ag/AgCl electrode. The noncontact electrode, through hair, shows more signal degradation and susceptibility to movement artifacts. However, the online experiments in this study demonstrate that both electrodes can be successfully utilized within controlled BCI applications.

Fundamentally, noncontact sensors make trade-off between ease of operation (no scalp preparation, through hair), signal quality (noise, movement artifacts) and sensor complexity. The poor coupling interface, through dry hair, accounts for much of the degradation in signal quality and appears to be intrinsic to the technology. Nevertheless, with careful circuit design, it is possible to still resolve EEG-level signals with noncontact sensors. It is hoped that the data and methods presented in this study establish a proof-of-concept baseline to generate further interest in noncontact EEG research towards building practical devices.

References

[1] C.-T. Lin, L.-W. Ko, J.-C. Chiou, J.-R. Duann, R.-S. Huang, S.-F. Liang, T.-W. Chiu, and T.-P. Jung, "Noninvasive neural prostheses using mobile and wireless EEG," *Proc. IEEE*, vol. 96, no. 7, pp. 1167–1183, Jul. 2008.

[2] Y.-T. Wang, Y. Wang, and T.-P. Jung, "A cell-phone-based brain computer interface for communication in daily life," *J. Neural Eng.* vol. 8, no. 2, p. 025018, 2011.

[3] U. Hoffmann, E. Fimbel, and T. Keller, "Brain-computer interface based on high frequency steady-state visual evoked potentials: A feasibility study," in *Int. IEEE/EMBS Conf. Neural Eng.*, May 2, 2009, pp. 466–469.

[4] W. Yijun, W. Ruiping, G. Xiaorong, and G. Shangkai, "Brain-computer interface based on the high-frequency steady-state visual evoked potential," in *Proc. 2005 1st Int. Conf. Neural Interface Control*, May 2005, pp. 37–39.

[5] Y. Wang, X. Gao, B. Hong, C. Jia, and S. Gao, "Brain-computer interfaces based on visual evoked potentials," *IEEE Eng. Med. Biol. Mag.*, vol. 27, no. 5, pp. 64–71, Sep.–Oct. 2008.

[6] Y. Wang, R. Wang, X. Gao, B. Hong, and S. Gao, "A practical vepbased brain-computer interface," *IEEE Trans. Neural Syst. Rehabil. Eng.*, vol. 14, no. 2, pp. 234–240, Jun. 2006.

[7] G. Bin, X. Gao, Z. Yan, B. Hong, and S. Gao, "An online multi-channel SSVEP-based brain computer interface using a canonical correlation analysis method," *J. Neural Eng.* vol. 6, no. 4, p. 046002, 2009.

[8] Y. Chi, T.-P. Jung, and G. Cauwenberghs, "Dry-contact and noncontact biopotential electrodes: Methodological review," *IEEE Rev. Biomed. Eng.*, vol. 3, pp. 106–119, 2010.

[9] G. Gargiulo, P. Bifulco, R. Calvo, M. Cesarelli, C. Jin, and A. van Schaik, "A mobile EEG system with dry electrodes," in *Proc. IEEE Biomed. Circuits Syst. Conf.*, Nov. 2008, pp. 273–276.

[10] G. Ruffini, S. Dunne, E. Farres, P. Watts, E. Mendoza, S. Silva, C. Grau, J. Marco-Pallares, L. Fuentemilla, and B. Vandecasteele, "Enobio—First tests of a dry electrophysiology electrode using carbon nanotubes," in *Proc. 28th Ann. Int. Conf. IEEE Eng. Med. Biol. Soc.*, Aug. 2006, pp. 1826–1829.

[11] G. Ruffini, S. Dunne, E. Farres, I. Cester, P. Watts, S. Ravi, P. Silva, C. Grau, L. Fuentemilla, J. Marco-Pallares, and B. Vandecasteele, "Enobio dry electrophysiology electrode; first human trial plus wireless electrode system," in *Proc. 29th Annu. Int. Conf. IEEE Eng. Med. Biol. Soc.*, 2007, pp. 6689–6693.

[12] T. Sullivan, S. Deiss, T.-P. Jung, and G. Cauwenberghs, "A brain machine interface using dry-contact, low-noise EEG sensors," in *IEEE Int. Symp. Circuits Syst. Conf.*, 2008, pp. 1986–1989.

[13] P. Griss, P. Enoksson, H. Tolvanen-Laakso, P. Merilainen, S. Ollmar, and G. Stemme, "Spiked biopotential electrodes," in *Proc. 13th Annu. Int. Conf. Micro Electro Mechan. Syst.*, 2000, pp. 323–328.

[14] J.-C. Chiou, L.-W. Ko, C.-T. Lin, C.-T. Hong, T.-P. Jung, S.-F. Liang, and J.-L. Jeng, "Using novel mems EEG sensors in detecting drowsiness application," in *IEEE Biomed. Circuits Syst. Conf.*, Nov. 2006, pp. 33–36.

[15] T. Sullivan, S. Deiss, and G. Cauwenberghs, "A low-noise, non-contact EEG/ECG sensor," in *IEEE Biomed. Circuits Syst. Conf.*, 2007, pp. 154–157.

[16] B. Alizadeh-Taheri, R. L. Smith, and R. T. Knight, "An active, microfabricated, scalp electrode array for EEG recording," *Sensors Actuators A: Physical* vol. 54, no. 1–3, pp. 606–611, 1996.

[17] B. A. Taheri, R. T. Knight, and R. L. Smith, "A dry electrode for EEG recording," *Electroencephalogr. Clin. Neurophysiol.* vol. 90, no. 5, pp. 376–383, 1994.

[18] P. Griss, H. Tolvanen-Laakso, P. Merilainen, and G. Stemme, "Characterization of micromachined spiked biopotential electrodes," *IEEE Trans. Biomed. Eng.*, vol. 49, no. 6, pp. 597–604, Jun. 2002.

[19] L.-D. Liao, P.-P. Chao, Y.-H. Chen, C.-T. Lin, L.-W. Ko, H.-H. Lin, and W.-H. Hsu, "A novel hybrid bioelectrode module for the zero-prep EEG measurements," in *IEEE Sensors*, Oct. 2009, pp. 939–942.

[20] R. Matthews, N. McDonald, P. Hervieux, P. Turner, and M. Steindorf, "A wearable physiological sensor suite for unobtrusive monitoring of physiological and cognitive state," in *Proc. 29th Annu. Int. Conf. IEEE Eng. Med. Biol. Soc.*, 2007, pp. 5276–5281.

[21] C.-T. Lin, L.-D. Liao, Y.-H. Liu, I.-J. Wang, B.-S. Lin, and J.-Y. Chang, "Novel dry polymer foam electrodes for long-term EEG measurement," *IEEE Trans. Biomed. Eng.*, vol. 58, no. 5, pp. 1200–1207, May 2011.

[22] J. R. Estepp, J. C. Christensen, J. W. Monnin, I. M. Davis, and G. F. Wilson, "Validation of a dry electrode system for EEG," in *Proc. Human Factors Ergonomics Soc. Annu. Meeting*, 2009, pp. 1171–1175.

[23] T. O. Zander, M. Lehne, K. Ihme, S. Jatzev, J. Correia, C. Kothe, B. Picht, and F. Nijboer, "A dry EEG-system for scientific research and brain-computer interfaces," *Frontiers Neurosci.*, vol. 5, 2011.

[24] A. S. Gevins, D. Durousseau, and J. Libove, "Dry electrode brain wave recording system," U.S. Patent 4 967 038, Oct. 30, 1990.

[25] C. J. Harland, T. D. Clark, and R. J. Prance, "Remote detection of human electroencephalograms using ultrahigh input impedance electric potential sensors," *Appl. Phys. Lett.* vol. 81, no. 17, pp. 3284–3286, 2002.

[26] M. Oehler, P. Neumann, M. Becker, G. Curio, and M. Schilling, "Extraction of SSVEP signals of a capacitive EEG helmet for human machine interface," in *Proc. 30th Annu. Int. Conf. IEEE Eng. Med. Biol. Soc.*, Aug. 2008, pp. 4495–4498.
[27] Y. Chi, C. Maier, and G. Cauwenberghs, "An integrated, low-noise, high input impedance front-end for non-contact BCI and BSN physiological monitoring systems," in *IEEE CAS-FEST: The 2011 Forum Emerging Selected Topics*, 2011.
[28] Y. Chi and G. Cauwenberghs, "Micropower non-contact EEG electrode with active common-mode noise suppression and input capacitance cancellation," in *Proc. Annu. Int. Conf. IEEE Eng. Med. Biol. Soc.*, 2009, pp. 4218–4221.
[29] J. Ottenbacher and S. Heuer2, "Motion artefacts in capacitively coupled ECG electrodes," *IFMBE Proc.*, vol. 25, no. 4, pp. 1059–1062, 2009.
[30] Y. Chi, C. Maier, and G. Cauwenberghs, "Integrated ultra-high impedance front-end for non-contact biopotential sensing," presented at the IEEE Biomed. Circuits Syst. Conf., San Diego, CA, 2011.
[31] J. R. Wolpaw, N. Birbaumer, D. J. McFarland, G. Pfurtscheller, and T. M. Vaughan, "Brain-computer interfaces for communication and control," *Clin. Neurophysiol.* vol. 113, no. 6, pp. 767–791, 2002.

Yu Mike Chi (S'96–M'00) received the B.S. degree in electrical engineering from the Johns Hopkins University, Baltimore, MD, in 2007, and the Ph.D. degree in electrical engineering from the University of California-San Diego, La Jolla, in 2011.

He is currently the Chief Technology Officer at Cognionics, Inc., working on wireless and noncontact biopotential sensing systems.

Yu-Te Wang received the M.S. degree from National Chiao Tung University, Hsinchu, Taiwan, in 2009. He is currently working toward the Ph.D. degree at the University of California-San Diego, La Jolla.

His research interests include software design and brain–computer interface.

Yijun Wang received his B.E. and Ph.D. degrees in biomedical engineering from Tsinghua University, Beijing, China, in 2001 and 2007, respectively.

Currently, he is a postdoctoral researcher at the Swartz Center for Computational Neuroscience, University of California San Diego. His research interests include brain–computer interface, biomedical signal processing, and machine learning.

Christoph Maier (S'04–M'11) received the Diplom-Physiker degree from the University of Heidelberg, Heidelberg, Germany, in 1995, and the Dr.sc. degree in electrical engineering from the Swiss Federal Institute of Technology, Zurich, Switzerland, in 2000.

After time in industry, he joined the Integrated Systems Neuroengineering laboratory at UCSD as postdoctoral researcher in 2010. His main research interests are interfaces for electrophysiological signals and modeling neural networks in analog VLSI.

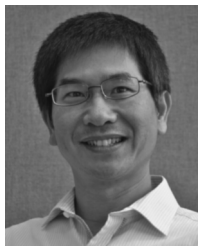

Tzyy-Ping Jung (S'91–M'92–SM'06) received the B.S. degree in electronics engineering from the National Chiao Tung University, Hsinchu, Taiwan, in 1984, and the M.S. and Ph.D. degrees in electrical engineering from The Ohio State University, Columbus, in 1989 and 1993, respectively.

He was a Research Associate of National Research Council, National Academy of Sciences, in 1993–1996. He is currently a co-Director of the Center for Advanced Neurological Engineering and an Associate Director of the Swartz Center for Computational Neuroscience, University of California-San Diego (UCSD). He is also an adjunct Professor of Department of Bioengineering at UCSD and Professor in the Department of Computer Science, National Chiao Tung University, Hsinchu, Taiwan. His research interests include areas of biomedical signal processing, cognitive neuroscience, machine learning, time-frequency analysis of human electroencephalogram, functional neuroimaging, and brain–computer interfaces and interactions.

Gert Cauwenberghs (S'89–M'94–SM'04–F'11) received the Ph.D. degree in electrical engineering from California Institute of Technology, Pasadena, in 1994.

He is a Professor of Bioengineering at University of California–San Diego, La Jolla, where he co-directs the Institute for Neural Computation. He previously held positions as Professor of Electrical and Computer Engineering at Johns Hopkins University, Baltimore, MD, and Visiting Professor of Brain and Cognitive Science at Massachusetts Institute of Technology, Cambridge. His research interests cover neuromorphic engineering, low-noise and low-power integrated biomedical instrumentation, neuron-silicon and brain-machine interfaces, computational and systems neuroscience, as well as learning and intelligent systems.

Dr. Cauwenberghs received the NSF Career Award in 1997, ONR Young Investigator Award in 1999, and Presidential Early Career Award for Scientists and Engineers in 2000. He serves as Associate Editor for IEEE TRANSACTIONS ON NEURAL SYSTEMS AND REHABILITATION ENGINEERING, Senior Editor for IEEE SENSORS JOURNAL and IEEE JOURNAL OF EMERGING TOPICS IN CIRCUITS AND SYSTEMS, and Editor-in-Chief for IEEE TRANSACTIONS ON BIOMEDICAL CIRCUITS AND SYSTEMS.